International Journal of Mechanical and Industrial Engineering

Volume 4 | Issue 1 Article 6

July 2014

COMPARISON OF VARIOUS NUMERICAL DIFFERENCING SCHEMES IN PREDICTING NON-NEWTONIAN TRANSITION FLOW THROUGH AN ECCENTRIC ANNULUS WITH INNER CYLINDER IN ROTATION

SATISH KUMAR DEWANGAN
National Institute of Technology; Raipur, C.G. (INDIA), satish_dewangan@yahoo.com

S.L. SINHA
National Institute of Technology, Raipur, C.G. (INDIA), shobha_sihna1@rediffmail.com

COMPARISON OF VARIOUS NUMERICAL DIFFERENCING SCHEMES IN PREDICTING NON-NEWTONIAN TRANSITION FLOW THROUGH AN ECCENTRIC ANNULUS WITH INNER CYLINDER IN ROTATION

SATISH KUMAR DEWANGAN[1] & S.L.SINHA[2]

[1]Assistant Professor, Applied Mechanics Department, National Institute of Technology; Raipur, C.G. (INDIA),
[2]Associate Professor, Mechanical Engineering Department, National Institute of Technology, Raipur, C.G. (INDIA)
E-mail: satish_dewangan@yahoo.com,shobha_sihna1@rediffmail.com

Abstract- Flow through annulus is a widely solved problem in fluid mechanics because of its practical applicability in many areas. In oil well drilling, cuttings generated are of non-Newtonian nature which flows through an eccentric annulus with inner cylinder in rotation, considering the real drilling situations. In the present work, a comparison have been done amongst three differencing schemes, the second order upwind, the Power law scheme and QUICK scheme used in computational fluid dynamics solution algorithms, so as to find the best amongst them to solve transition flow for this case as well as in general. A three dimensional orthogonal hexahedral mesh with suitable boundary conditions & input parameters was taken as computational domain for eccentric annulus. This was solved with standard k-ω turbulence model and SIMPLE algorithm. Results were validated against the published experimental work of J. M. Nouri, et. al [1]. Radial velocity, axial velocity and tangential velocity of fluid were plotted along chosen planes and contours of molecular viscosity as well as turbulence kinetic energy were observed for comparison amongst the solutions obtained by three differencing schemes. Although in most of the cases close agreement have been observed between computational data, but as far as prediction of radial velocity is concerned there was surprising difference amongst the three schemes.

Keywords- *Non-Newtonian Flow; Transition Flow; Eccentric Annulus.*

I. INTRODUCTION

Flow through annulus is a widely solved problem. Chemical process & petroleum industries, Pipeline engineering, Power plants, Biomedical engineering applications, Micro scale fluid dynamics studies, Food processing industries, geothermal flows, extrusion of molten plasticsetcencounter many applicable situations of flow through such geometrical situation of concentric annulus or eccentric annulus. A large variety of fluids and industrial applications has been a major motivation for research in annular flow with varying degrees of complexity. An extensive bibliographic list of work on annular flows has been presented by Escudier et al. [2]. Of concern to this work are mainly previous investigations with viscoelastic fluids in concentric annuli under laminar flow conditions.

Usual situation occurring in the case of oil well and gas well drilling mud flow is either transition or turbulent situation. In the work of J.M. Nouri [1] et al. three velocity components (axial, radial and tangential) of a Newtonian and a weakly elastic shear-thinning non-Newtonian fluid have been measured in an annulus with an eccentricity of 0.5, a diameter ratio of 0.5, and an inner cylinder rotation of 300 rpm. The results show that the rotation had similar effects on the Newtonian and non-Newtonian fluids, with a more uniform axial flow across the annulus and the maximum tangential velocities in the narrowest gap in both cases. The turbulence intensities in the region of widest gap were uninfluenced by rotation, increased in the Newtonian fluid, and - decreased in the non-Newtonian fluid in the region of the smallest gap. D.O.A. Cruz et. al. [3] has obtained analytical solution of helical flow of fluids in concentric annuli due to inner cylinder rotation as well for Poiseuille flow in a channel skewed by the movement of one plate in span wise direction, which constitutes a simpler solution for helical flow in the limit of very thin annuli. Expressions are derived for the radial variation of the axial and tangential velocities, as well as for the three shear stresses and the two normal stresses using non dimensional no as Reynolds No and Taylor No etc.I. A. Frigaardet. al. [4] has worked in predicting the rheological properties that are necessary to prevent the annular plug fluid from flowing under the action of buoyancy, or indeed to predict how far the plug material may flow for given rheological properties for annular fluid flow in oil wellbore construction. Mathematically, these flows were modelled using a Hele-Shaw approximation of the narrow annulus. V. C. Kelessidis (SPE) et. al. [5] has presented a critical review of the state-of-art modelling for efficient cutting transport during Coiled-tube drilling, and presented the critical parameters like pump rate, well dimension, fluid sizes, solid loading and hole inclination etc affecting efficient cutting transport. They set up a laboratory system also. M. P. Escudieret. al. [6] reports experimental data for fully developed laminar flow of a shear-thinning liquid through both a concentric and an 80% eccentric annulus with and without centre body rotation. The working fluid was an aqueous solution of 0.1% xanthan gum and 0.1% carboxy-

methyl cellulose. A. A. Gavrilovet. al. [10] proposed a numerical algorithm for simulating steady laminar flows of an incompressible fluid in annular channels with eccentricity and rotation of the inner cylinder. The algorithm enabled description of this class of flows for wide ranges of the annular channel and flow parameters. For a series of flows in an annular clearance, these numerical results were compared with the available analytic solutions and experimental data. The simulated data agree well with the available experimental, analytical, and numerical solutions.Sang-Mok Hanet. al. [11] investigated hydraulic transport characteristics of a solid-liquid mixture flowing vertically upward where solid particles are carried by non-Newtonian fluids in a slim hole concentric annulus with rotating inner cylinder. Solid volumetric concentration and pressure drops were measured for the various parameters such as inclined annulus, flow rate, and rotational speed of inner cylinder. Aqueous solution of sodium carboxymethyl cellulose 0.2 ~ 0.4% CMC) and 5% bentonite solutions were taken for non Newtonian fluid one by one. For both CMC and bentonite solutions, the higher the concentration of the solid particles are, the larger the pressure drops become.Wang Zhiyuan [12] established the basic hydrodynamic models, including mass, momentum, and energy conservation equations for annular flow with gas hydrate phase transition during gas kick for deep water drilling.They investigated the behaviour of annular multiphase flow with hydrate phase transition by analyzing the hydrate-forming region, the gas fraction in the fluid flowing in the annulus, pit gain, bottom hole pressure, and shut-in casing pressure. Results show that it is possible to move the hydrate-forming region away from sea floor by increasing the circulation rate. The decrease in gas volume fraction in the annulus due to hydrate formation reduces pit gain, which can delay the detection of well kick and increase the risk of hydrate plugging in lines. Caution is needed when a well is monitored for gas kick at a relatively low gas Production rate, because the possibility of hydrate presenceis much greater than that at a relatively high production rate. The shut-in casing pressure cannot reflect the gas kick due to hydrate formation, which increases with time. Young-Ju Kim et. al [13] did an experimental investigation concerning the characteristics of vortex flow in a concentric annuluswith a diameter ratio of 0.52, whose outer cylinder is stationary and inner one is rotating. Pressure losses and skin friction coefficients have been measured for fully developed flows of water and of 0.4~o aqueous solution of sodium carboxy-methyl cellulose (CMC), respectively, when the inner cylinder rotates at the speed of 0--600 rpm. Also, the visualization of vortex flows has been performed to observe the unstable waves. E. V. Podryabinkinet. al. [14] presents results of numerical modeling for analysis of the moment and forces exerted on an eccentrically positioned rotating inner cylinder due to the annular flow between two cylinders with parallel axes. Laminar stationary fully developed flows of Newtonian and power law fluid flows are considered. An impact of annulus geometry, flow regime, and fluid characteristics are studied. The study indicates that the moment exerted on the inner cylinder increases monotonically with the eccentricity. Forces acting on the inner cylinder include pressure and viscous friction. The pressure forces provide a predominant contribution. When eccentricity does not exceed a certain critical value, the radial force pushes the inner cylinder to the channel wall. When eccentricity is large enough, the radial force reverses its sign, and the inner cylinder is pushed away from the outer wall. Circumferential component of the force has always the same direction and induces precession of the inner cylinder. Sang-mokHan [15] experimentally studied solid-liquid mixture upward hydraulic transport of solid particles in vertical and inclined annuli with rotating inner cylinder. Effect of annulus inclination and drill pipe rotation on the carrying capacity of drilling fluid, particle rising velocity, and pressure drop in the slim hole annulus have been measured for fully developed flows of water and of aqueous solutions of sodium carboxy methyl cellulose (CMC) and bentonite, respectively. For higher particle feed concentration, the hydraulic pressure drop of mixture flow increases due to the friction between the wall and solids or among solids. In these researches, depending upon the type and nature of the flow different solution methodology has been adopted. Usually turbulent & transitional non-Newtonian flows are often encountered in the oil and gas industry. These fluids are used in the drilling of oil wells to transport the cuttings to the surface, and to keep solids in suspension during stationary periods.

In directional drilling, an eccentric annulus is often used, there is a tendency for the cuttings to accumulate in the narrowest gap where the velocity is lowest. The cutting generated is of Non-Newtonian nature. And although the cutting is a directional process, still along with the axial annular flowinvolves lateral rotational effects because of the rotation of inner cylindrical portion of the annulus. Such combination of axial annulus flow along with the lateral rotation brings the flow in that zone to be in transition or in turbulence state. This tends to suppress such accumulation of cuttings. Thus it is very much important to maintain transition or turbulent flowsituation. This, in turn, requires knowledge of the velocity profiles and other flow characteristics in the annulus as essential in the proper design and operation of the drills.

In computational solution procedure, while solving such problems selection of proper turbulence model, selection of properpressure – velocity coupling resolution methodand type of descretization schemes for flow are very essential. There are various upwind schemes to capture the flow effects depending on the dominance of flow direction & magnitude. When flow of fluid plays a significant role, the convection effects of flow must be taken into account while solving these conservation equations for boundary conditions given in a problem under consideration.

This requires selection of right type of differencing scheme for the flow properties &other variables (i.e. momentum terms, pressure, turbulence kinetic energy etc) involved. The various differencing schemes for predicting convective effects of flow are; upwind scheme, Power law schemes and QUICK scheme etc., (in the increasing order of effectiveness). Upwind differencing scheme is simple & thus can be extended to multidimensional problems but has a drawback that it produces erroneous results when the flow direction is not aligned with grid lines. The upwind differencing scheme causes the distributions of the transported properties to become smeared & cause false diffusion. Power law scheme is fully conservative, unconditionally bounded is highly stable & produces realistic solutions. This scheme is very useful in predicting practical flows QUICK scheme has very small false diffusion problem and the solution achieved with coarse grids are often considerably more accurate those of former schemes. Thus effectiveness of these differencing schemes in capturing the convection effects is judged by how far they are able to satisfy the three qualities namely Conservativeness, Bounded-ness and Transportiveness. H. K. Versteeg et al. [7].

The objective of the present study is to investigate the flow prediction effectiveness of second order upwind and power law differencing schemes, in respect to QUICK schemes for case of eccentric annulus (Refer Table 1 for model details) non-Newtonian flow with inner cylinder rotation. Before it, the results of QUICK scheme have been verified by comparing them with that of experimental data for the case considered. Three dimensional and two dimensional (mid-plane of the annulus normal to the annulus axis) representation of the geometry is shown in Figure 1& Figure 2 respectively.

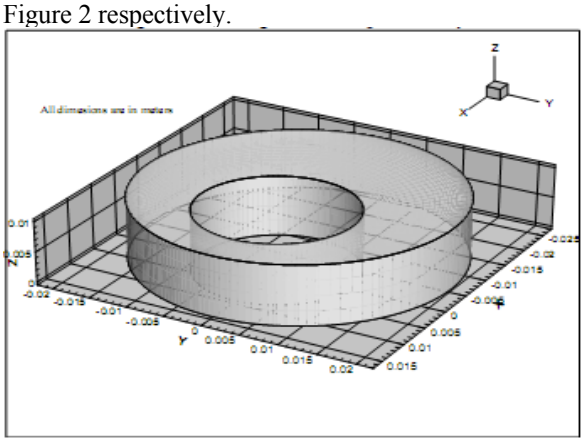

Figure (1): Three Dimensional Representation of the Eccentric Annulus

Table 1: Model Details: Reference [8]

CylinderDiameter (D_i)	= 20mm
Outer cylinder Diameter(D_O)	= 40.3 mm
Max hydraulic mean diameter ($D_h)_{max}$	= 20.3 mm
Maximum Eccentricity e_{max}	= 5.15 mm.
Axial dimension for the cylinders	= 10 mm
Inner cylinder is in clockwise rotation with 300 rpm.	
Outer cylinder is fixed.	
Centre of the innercylinder is taken as reference centre for measurement of the eccentricity.	

Flow is considered to be three dimensional, incompressible, steady &in transition with Bulk axial Reynolds no (Re) equal to 9000.The flow direction is along positive z-axis, through the eccentric annulus of flow between the cylinders. Axial mass flow rate (m) & axial bulk velocity (U) corresponding to the chosen Reynolds no was 2.615 kg/s and 2.72 m/s, which were calculated using the following relations;

Axial Bulk velocity; $U = (R_e \times D_H \times \rho) / \mu_{wall}$; and

Axial mass flow rate; $m = U \times A \times \rho$.

Where $A = (\pi/4)(D_O^2 - D_I^2)$, and $\mu_{wall} = 6 \times 10^{-3}$ measured experimentally by J. M. Nouriet. al. [1]

Table 2: Non-Newtonian power law parameters

Power law index (n)	=	0.75
consistency index (K)	=	0.044
Minimumviscosity Limit ( )	=	
0.0001kg/m-sMaximum Viscosity Limit ( )		
= 1000 kg/m-s		
Reference Temperature	=	310 K

The values of these non-Newtonian power law parameters for test fluid used in this study were obtained from the dataprescribed by J. M. Nouriet. al. [1].

The numerical formulation is based on the finite volume method as implemented in ANSYS-FLUENT 12. SIMPLE algorithm has been applied for dealing with pressure velocity coupling. The present study employs standard k-omega turbulence model with transition flow option & shear flow corrections.

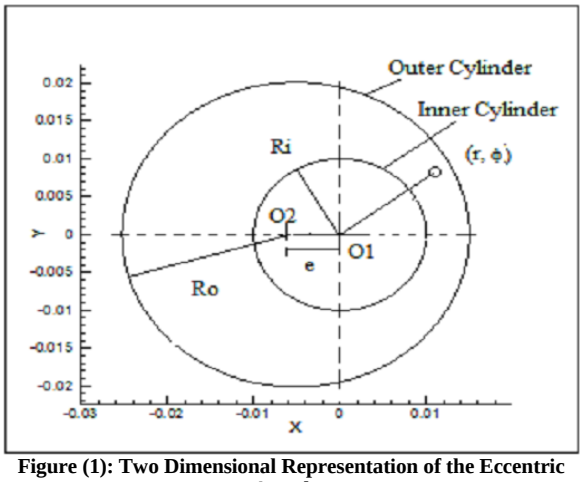

Figure (1): Two Dimensional Representation of the Eccentric Annulus

II. MATHEMATICAL AND NUMERICAL FORMULATION

In the present work, flow has been modelled as three dimensional, incompressible, Transition flow of Non-Newtonian fluid. ANSYS-FLUENT solves the problem using conservation equations as guideline. Flow of fluid is governed by the Navier–Stokes equation and continuity equations. The coordinate-

freetime averaged form of the Navier-Stokes equations(K. Muralidhar et. al. [9]) is being given below;

$$\rho\left(\frac{\partial\bar{\bar{U}}}{\partial\tau}+\bar{U}.\nabla\bar{U}\right)=-\nabla p+\mu\nabla^2\bar{U}+\nabla.\sigma_T$$

Time averaged velocity components of turbulent flow satisfy the same Navier-Stokes equation as for laminar flow, provided the laminar stresses are increased by additional stress known as apparent stresses of turbulent flow or Reynolds stresses. These are given by symmetric stress tensor as below;

$$\sigma_T=\begin{bmatrix}\overline{U'^2_r} & \overline{U'_rU'_t} & \overline{U'_rU'_a}\\ \overline{U'_rU'_t} & \overline{U'^2_t} & \overline{U'_tU'_a}\\ \overline{U'_rU'_a} & \overline{U'_tU'_a} & \overline{U'^2_a}\end{bmatrix}$$

Details of velocity vectorU and Del operators in radial coordinates are as below;

$$\bar{U}=\bar{U}_re_r+\bar{U}_te_t+\bar{U}_ae_a;\qquad \nabla=\left(e_r\frac{\partial}{\partial r}+\frac{e_t}{r}\frac{\partial}{\partial t}+e_a\frac{\partial}{\partial a}\right)$$

$$\nabla^2=\nabla.\nabla=\left(\frac{\partial^2}{\partial r^2}+\frac{1}{r}\frac{\partial}{\partial r}+\frac{1}{r^2}\frac{\partial^2}{\partial t^2}+\frac{\partial^2}{\partial a^2}\right)$$

$$\nabla^2\bar{U}=(\nabla^2\bar{U}_r,\nabla^2\bar{U}_t,\nabla^2\bar{U}_a)+\frac{1}{r^2}\frac{\partial^2}{\partial t^2}\bar{U}$$

The second term is:

$$\left(\frac{\partial^2\bar{U}_r}{\partial t^2}-U_r-2\frac{\partial\bar{U}_t}{\partial t}\right)e_r+\left(\frac{\partial^2\bar{U}_t}{\partial t^2}+2\frac{\partial\bar{U}_r}{\partial t}-\bar{U}_t\right)e_t$$

The nonlinear acceleration term would be;

$$\bar{U}.\nabla\bar{U}=e_r\left(\bar{U}r\frac{\partial\bar{U}_r}{\partial r}+\frac{U_t}{r}\frac{\partial\bar{U}_r}{\partial t}-\frac{\bar{U}_t^2}{r}+U_a\frac{\partial\bar{U}_r}{\partial a}\right)+e_t\left(\bar{U}r\frac{\partial\bar{U}_t}{\partial r}+\frac{\bar{U}_r\bar{U}_t}{r}+\frac{\bar{U}_t}{r}\frac{\partial\bar{U}_t}{\partial t}+U_a\frac{\partial\bar{U}_t}{\partial a}\right)+e_a\left(\bar{U}r\frac{\partial\bar{U}_a}{\partial r}+\frac{U_t}{r}\frac{\partial\bar{U}_a}{\partial t}+U_a\frac{\partial\bar{U}_a}{\partial a}\right)$$

continuity equation for the incompressible fluid is given as under;

$$\nabla.\bar{U}=\left(\frac{\partial\bar{U}_r}{\partial r}+\frac{\bar{U}_r}{r}+\frac{1}{r}\frac{\partial\bar{U}_t}{\partial t}+\frac{\partial\bar{U}_a}{\partial a}\right)=0$$

Writing the Navier–Stokes equations in this form, allows the flexibility to use arbitrary non-Newtonian fluid model.Energy Conservation equation will not play any role since thermal parameters are not varying.

ANSYS-FLUENT provides four options for modelling non-Newtonian flows: (a) power law model, (b) Carreaau model for pseudo-plastics, (c) Cross model and (d) Herchel-Bulkey model for Bingham plastics. The test fluid is of Non-New to nian type.It has been described by power law model and represented by (when temperature is not involved in the case under study) the following equation;

$$\mu=K\ \gamma^{n-1}\qquad\text{---------- (3)}$$

Where viscosity μ has upper& lower limits as mentioned below;

$$\mu_{min}<(\mu=K\ \gamma^{n-1})<\mu_{max}$$

Here, K is the measure of the average viscosity of the fluid (the consistency index); n is a measure of the deviation of the fluid from Newtonian state (the power law index). If viscosity computed from the power law crosses these maximum or minimum limits then extreme value of that side will be used instead for calculation. The value of n determines the class of the fluid:

n = 1 -------- Newtonian Fluid
n> 1 --------- Shear thickening (dilatants fluid)
n< 1 ---------- Shear thinning (pseudo plastics)

Input parameter values for non-Newtonian fluid are already mentioned in the Table 2.

In the present work, three dimensional orthogonal mesh was used with total 20000 hexahedral cells. Two dimensional representation of the grid is shown in the Fig 3.

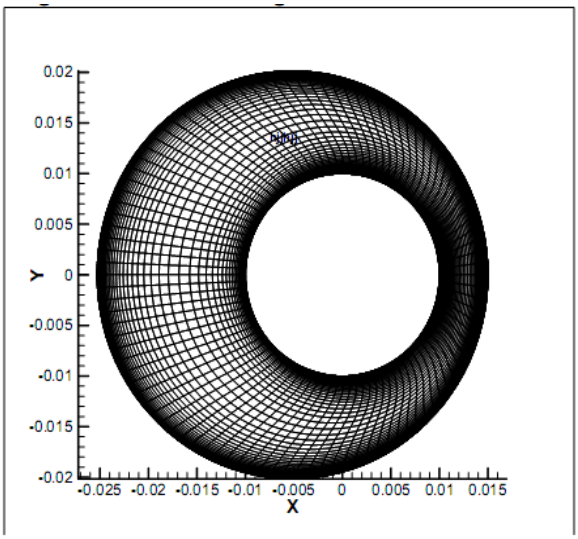

Figure (3): Two Dimensional View of the Eccentric Annulus Mesh

The following Boundary conditions have been specified for solving the different parameters in the domain;

(a) Periodic boundary condition along axial direction at the end faces, with mass flow rate input at z = 0.

(b) Moving wall boundary condition at the inner wall with clockwise rotation at constant angular velocityΩ;

(c) Stationary wall boundary condition at the outer wall.

No slip conditions are applicable at the both walls.
The Mesh, model details and boundary conditions were directly taken from the ANSYS- 12 user guide & manual [reference 8].

ANSYS-FLUENT 12 [reference 8] offers nine different turbulence models to capture the transition & turbulence effects in the flow. Since the present flow situation possibly lies in the transition flow situation thus standard K – ω (Turbulence Kinetic

Energy – Specific dissipation rate) model was adopted. This incorporated the modifications for shear flow corrections and low Reynolds number effects (within turbulence).

SIMPLE algorithm has been used for pressure velocity coupling. ANSYS – FLUENT12 [reference 8] uses a multi-grid scheme to accelerate the convergence of the solver by computing the corrections on a series of coarse grid levels. The use of multi-grid scheme can greatly reduce the number of iterations and the computational time required to obtain the converged solution.

A residual convergence of 10-6 has been obtained for the governing variables viz, mass balance, and velocitycomponents of the flow, k and ω. Under relaxation parameters were kept moderate and constant throughout the solution as mentioned in Table 3 below.

Table 3: Under Relaxation Parameters

Parameters;		Value
Pressure	:	0.3
Momentum	:	0.7
Density	:	1
Body Forces	:	1
Turbulent Kinetic Energy	:	0.8
Turbulence Viscosity	:	1
Specific Dissipation Rate	:	0.8
Energy	:	1

For representation of the results the calculated values will be displayed on defined planes p1, p2 and p3. The three planes are at locations of 3 o'clock, 12 o' clock and 9 o'clock corresponding to analogy with hour-arm of watch with respect to geometry under study. These locations are depicted in the Figure 4 and Table 4 as below.

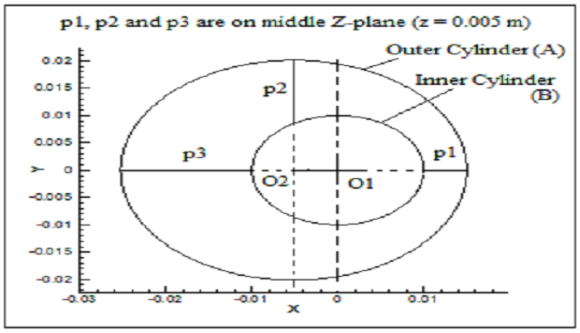

Figure (4): Representation of reference locations p1, p2 and p3 for eccentric annulus model

Table 4: Coordinate Locations of p1, p2 and p3

Plane	Coordinate	Min Extent (m)	Max Extent (m)
P1	X	0.01 m	0.015 m
	Y	0.00 m	0.00 m
	Z	0.005 m	0.005 m
P2	X	- 0.00515 m	- 0.00515 m
	Y	0.008566585 m	0.02015 m
	Z	0.005 m	0.005 m
P3	X	- 0.0253 m	- 0.01m
	Y	0.00 m	0.00 m
	Z	0.005 m	0.05 M

The results obtained were normalised only for the purpose of plot presentation of the results and that only of the velocity values.All velocity values were normalised with respect to inlet velocity as given below;

$$U_{an} = \frac{U_a}{U_{inlet}}; U_{tn} = \frac{U_t}{U_{inlet}}; \; and U_{rn} = \frac{U_r}{U_{inlet}}.$$

Distances along reference planes p1, p2 and p3 for plotting were normalised with respect to the dimension of eccentricity along these respective planes. These are;

$$p1_{nX} = \frac{p1_{X(max)} - p1_X}{p1_{X(max)} - p1_{X(min)}} = \frac{0.015 - p1_X}{0.005}$$

$$p2_{nY} = \frac{p2_{Y(max)} - p2_Y}{p2_{Y(max)} - p2_{Y(min)}} = \frac{0.02015 - p2_Y}{0.012}$$

$$p3_{nX} = \frac{p3_X - p3_{X(\min)}}{p3_{X(max)} - p3_{X(min)}} = \frac{p3_X - (-0.0253)}{0.0153}$$

Here, subscripts 'max' and 'min' indicate the respective maximum and minimum values as mentioned in the Table 4.

III. VALIDATION

The predicted flow field is validated against the experimental data by J. M. Nouriet. al [1]. For this, axial velocity (Ua) and tangential velocity (Ut) values were chosen. These were plotted along the three specified planes p1, p2 and p3 with respect to geometry under study. These locations are depicted & detailed in the Figure 4 and Table 4. All velocity values and the specified planes have been normalised (already discussed) for the representation.

Figure 5 says that the comparison between experimental and numerical result (by QUICK scheme) for variation of the axial velocity in the annular gap along the plane p1. There is qualitative match found between the experimental and numerical solutions, and have same trend of variation of axial velocity. Figure 6 is representing the comparison between the Experimental and Numerical results (by QUICK Scheme) for variation of the tangential velocity along the plane p1. Results by the two methods are following the same trend of variation of tangential velocity values. Both results are satisfying the physical situation of the problem as well. Figure 7 and Figure 9 are representing the axial velocity variation along planes p2 and p3 respectively for experimental and numerical results (by QUICK scheme). Figure 8 and Figure 10 are representing the tangential velocity variation along planes p2 and p3 respectively for experimental and numerical results (by QUICK scheme). By visual examination a qualitative match in the trend of velocity variation can be seen in these results also.

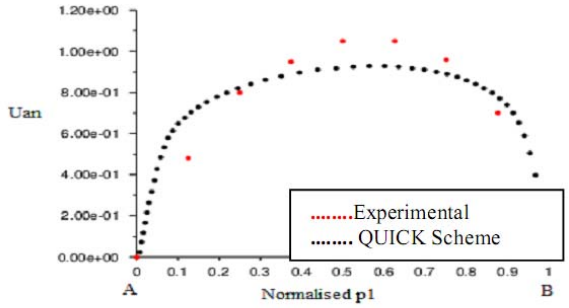

Figure (5): Comparison between experimental &results obtained by QUICK scheme for Axial velocity variation along p1

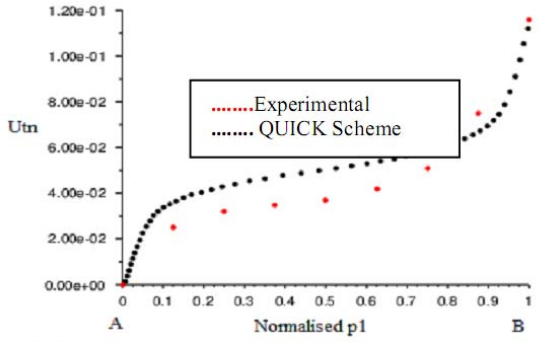

Figure (6): Comparison between experimental &results obtained by QUICK scheme for Tangential velocity variation along p1

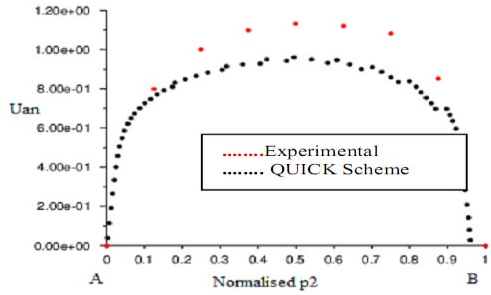

Figure (7): Comparison between experimental &results obtained by QUICK scheme for Axial velocity variation along p2

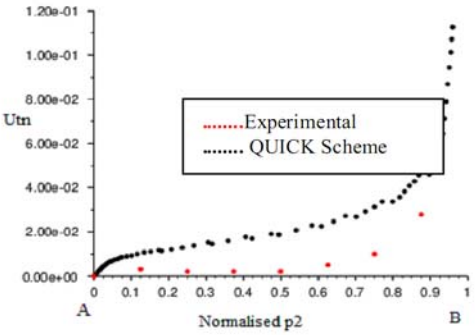

Figure (8): Comparison between experimental &results obtained by QUICK scheme for Tangential velocity variation along p2

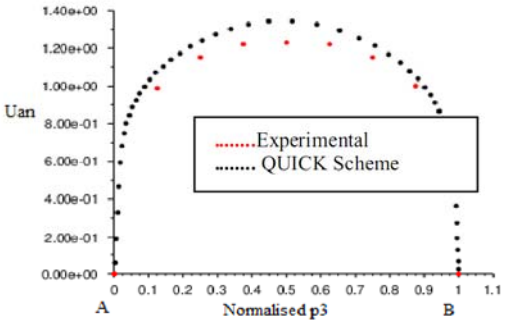

Figure (9): Comparison between experimental &results obtained by QUICK scheme for Axial velocity variation along p3

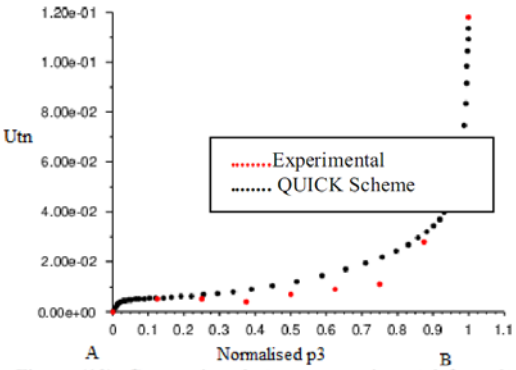

Figure (10): Comparison between experimental &results obtained by QUICK scheme for Tangential velocity variation along p3

The computed and experimental results are observed to be in good agreement.

IV. RESULTS AND DISCUSSIONS

The detailed results of the flow are presented using different types of differencing schemes viz. second order upwind, Power law differencing scheme and QUICK differencing scheme. Axial velocity, Radial velocity and Tangential velocity values of fluid particles were plotted for these three different schemes and compared with experimental data in Figure 5 to 10. Also contours for molecular velocity variation and turbulence kinetic energy variation, at middle z- plane (i.e. at z = 0.005 m) of the modelfor

various schemes have been presented in Figure 11 – 19. These physical quantities are very crucial in transition flow study for Transition non-Newtonian fluid flow. Molecular viscosity contours, figure 11 – 13, indicate that its value is maximum at around middle of the annular gap, at all values of the radial coordinate. Then, as wall is being approached may it be inner part of outer cylinder (which is stationary) or outer portion of the inner cylinder (which is in rotation at constant angular speed) molecular viscosity is approaching its minimum value. Molecular viscosity varies in the similar fashion as dynamics viscosity. Thus molecular viscosity is inversely proportional to rate of shear strain. Since for a transition flow situation, in the middle portions of the flow gaps shear strain rate is least in value thus naturally this results in maximum value of the molecular viscosity value.

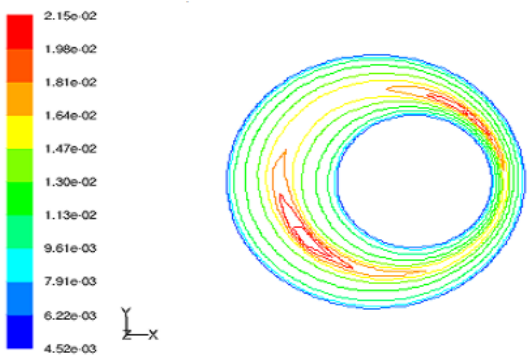

Figure (11): Molecular Viscosity Contours by Power Law Differencing Scheme

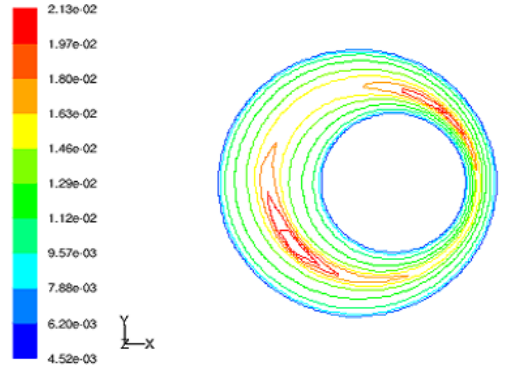

Figure (12): Molecular Viscosity Contour by QUICK Differencing Scheme

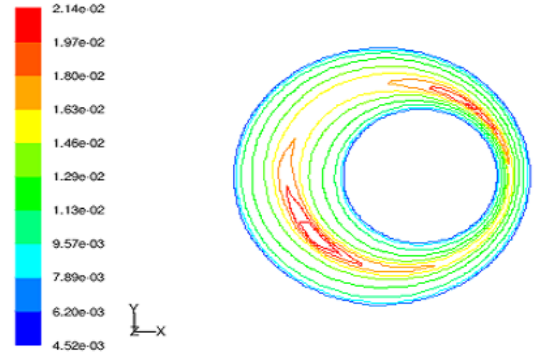

Figure (13): Molecular Viscosity Contours by Second Order Upwind Scheme

Turbulence kinetic energy (TKE) is the mean kinetic energy per unit mass associated with eddies in turbulent flow. Physically, the turbulence kinetic energy is characterised by measured root-mean-square (RMS) velocity fluctuations. In Reynolds-averaged Navier Stokes equations, the turbulence kinetic energy can be calculated based on the closure method, i.e. a turbulence model. Generally, the TKE can be quantified by the mean of the turbulence normal stresses:

$$k = \frac{1}{2}\{(\overline{U_a'})^2 + (\overline{U_t'})^2 + (\overline{U_r'})^2\}$$

Normal stress values being very small (as the fluctuating components of velocities being very small) turbulence kinetic energy will be small or vice versa. As indicated by the turbulence kinetic energy contours, Figure 14 – 16, being maximum near walls and reduces to minimum while proceeding towards middle portions of the eccentric gap at whichever radial direction considered. This shows that at these portions normal stress values and so fluctuating components of velocities and thus shear stress values will be maximum or minimum at those respective portions of the flow field.

Now as per the above discussion, when comparing the molecular viscosity contours, Figure 11 – 13, and turbulence kinetic energy contours, Figure 14 – 16, the two results are very well consistent as per the theory of fluid dynamics.

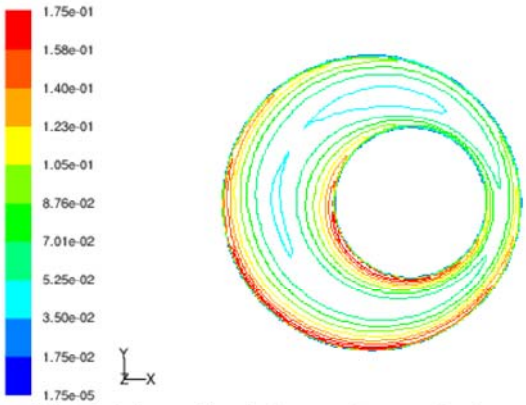

Figure (14): Turbulence Kinetic Energy Contours by Power Law Scheme

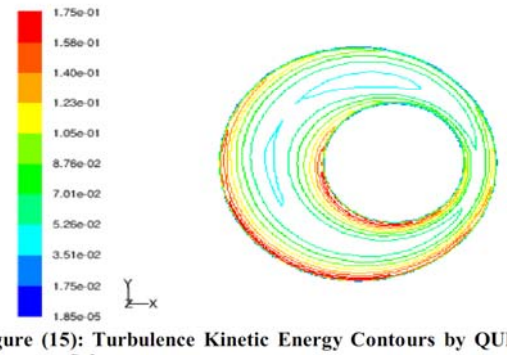

Figure (15): Turbulence Kinetic Energy Contours by QUICK Scheme

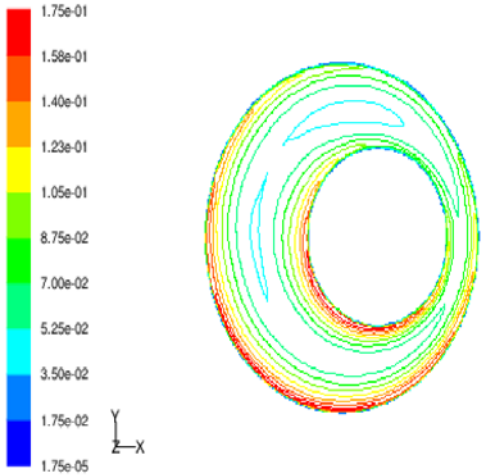

Figure (16): Turbulence Kinetic Energy Contours by Second Order Upwind Scheme

Axial velocity contours, Figure 17 – 19, indicate maximum values of it at lower part of the maximum eccentric gap in the flow domain. Now, proceeding towards the walls, it approaches zero velocity value satisfying the no-slip criterion at the solid boundaries because none of the cylinders is in axial motion (even though inner cylinder is in rotation).

Contour plots, from Figure 11 to 19, indicate that there is no significant difference found amongst the plots obtained by the three chosen schemes i.e. Power law scheme, QUICK scheme and second order upwind scheme. Qualitatively i.e. in terms of variation trend on the chosen plane (z = 0.005) all three schemes match. Of course in terms of the range (Maximum to minimum value) of the value there is very slight difference, whether the case is of molecular viscosity contours or of turbulence kinetic energy contours or that of axial velocity.

In some cases, these results of any 'two' schemes (different 'two' in different cases) are matching.

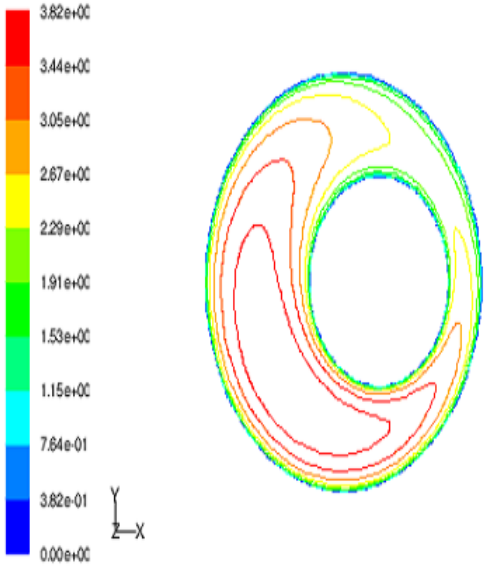

Figure (17): Axial Velocity Contours by Power Law Scheme

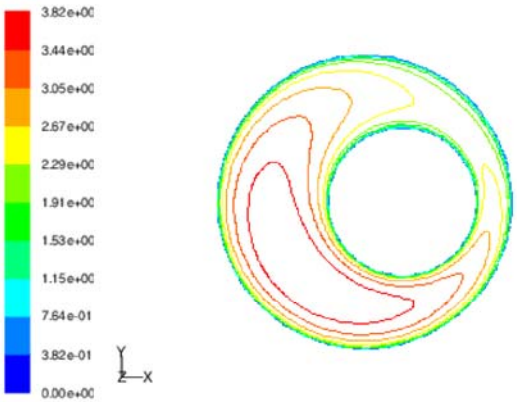

Figure (18): Axial Velocity Contours by QUICK Scheme

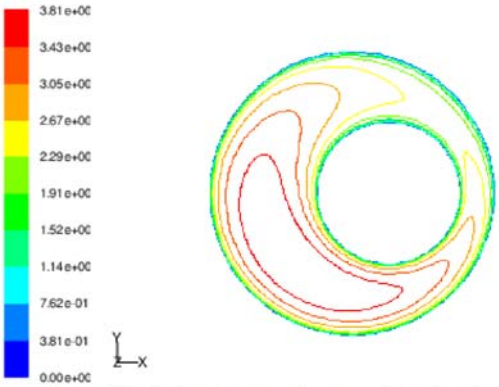

Figure (19): Axial Velocity Contours by Second Order Upwind Scheme

Figures 20 – 22 indicates comparison amongst three chosen differencing schemes for variation of axial velocity (Uan) along the p1, p2 and p3 planes, respectively. Similarly Figures 23 – 25 indicate radial velocity (Urn) variation and Figures 26 – 28 indicate tangential velocity (Utn) variation along the defined planes.

Axial velocity values are zero at inner and outer cylinders and between them follow parabolic profiles in the annulus gap. All the three schemes give very close match in relation to axial velocity distribution. Tangential velocity varies from zero at outer cylinder which is fixed to maximum value at the inner cylinder rotating at a constant speed of rotation. Again, like axial velocity distribution, tangential velocity distributions by all the three schemes are also in close agreement.Radial velocity distribution shows surprisingly different prediction for different schemes. For all the three radial velocity distributions i.e. along p1, p2 and along p3, one common point to note is that 2nd order upwind predictions are more close to QUICK predictions, whereas Power law scheme predictions are quite off the Quick. Of course this difference between schemes are significant for distance coordinates (i.e. normalised p1, normalised p2 and normalised p3) of value 0.4, being maximum at around 0.1, approximately – when proceeding from outer cylinder (A) towards inner cylinder (B). After distance coordinate of 0.4 differences between the predicted radial velocity values reducesfor the

schemes.Although magnitude wise there is difference, but variation of radial velocity for different schemes are following similar pattern.

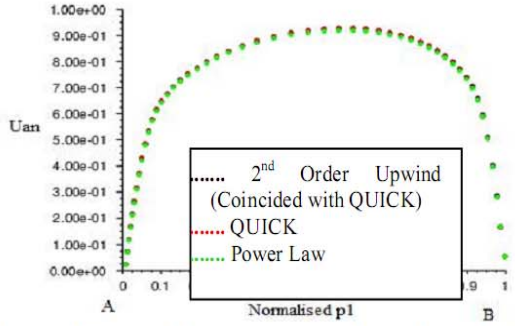

Figure (20): Axial Velocity variation along p1 for different schemes

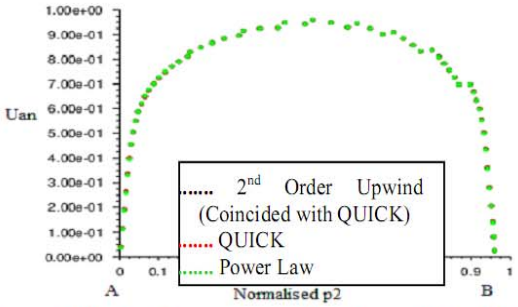

Figure (21): Axial velocity variation along p2 for different schemes

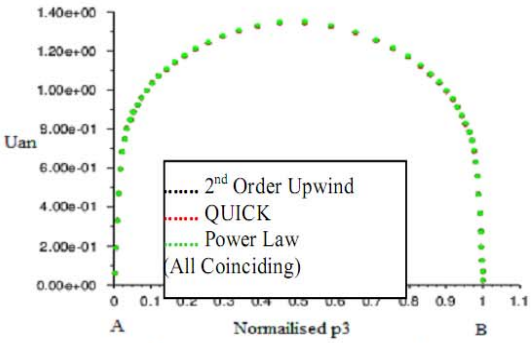

Figure (22): Axial velocity variation along p3 for different schemes

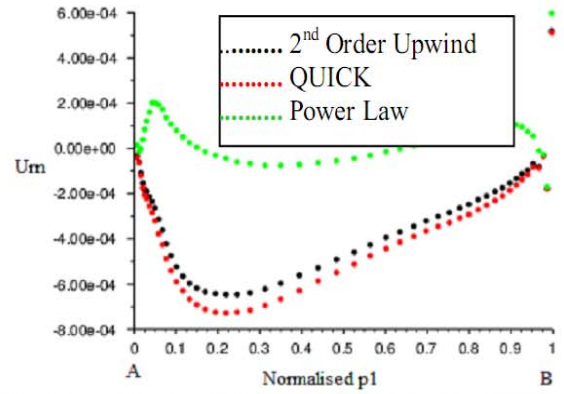

Figure (23): Radial velocity variation along p1 for different schemes

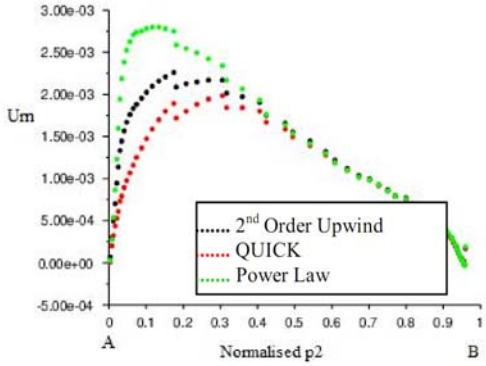

Figure (24): Radial velocity variation along p2 for different schemes

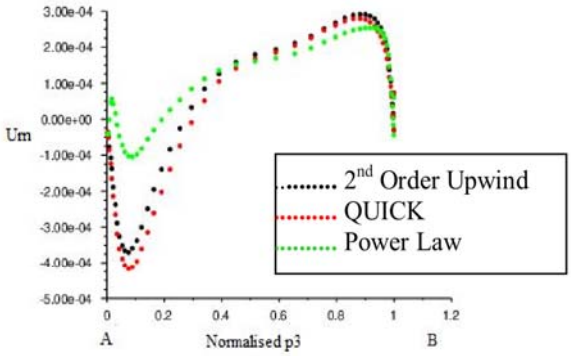

Figure (25): Radial velocity variation along p3 for different schemes

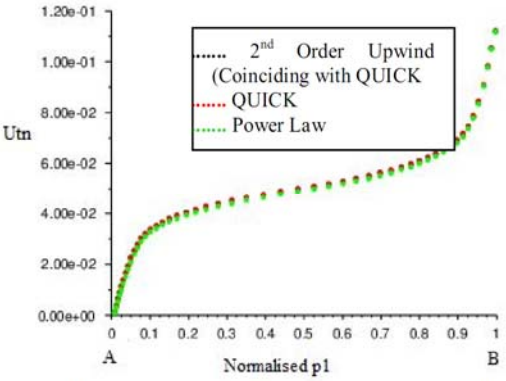

Figure (26): Tangential velocity variation along p1 for different schemes

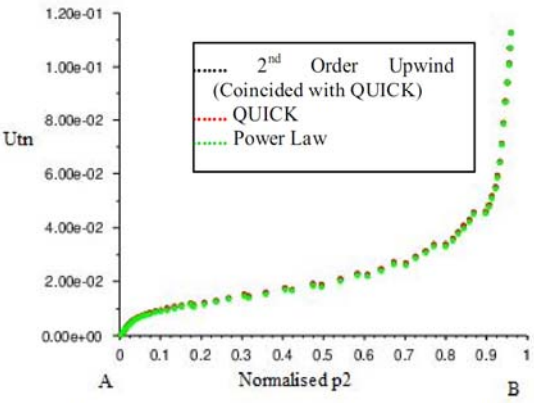

Figure (27): Tangential velocity variation along p2 for different schemes

Figures 23 – 25, which are representing radial velocity variation along p1 and p3 respectively are showing the possibility of radial flow reversals by observing the predictions of QUICK and 2nd order upwind schemes, where as that of power law this possibility looks very less. This nature is quite surprising, firstly in the sense that why there is no flow reversal possibility along p2, and secondly in the sense that although power law is considered to be of accuracy between 2nd order and QUICK still it lagged behind in capturing the convective effects of flow. These are the points to be focussed upon.

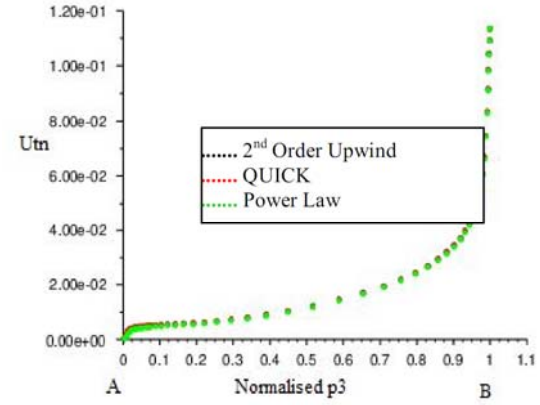

Figure (28): Tangential velocity variation along p3 for different schemes

V. CONCLUSION

This paper started with the objective of predicting the effectiveness of second order upwind and power law differencing scheme in respect to QUICK scheme for non Newtonian fluid flow through an eccentric annulus.

In this, for speed of rotation of 300 rpm under a constant Reynolds no 9000 flow of a test fluid (of non Newtonian in nature as found that of drilling mud) was considered. Results are very encouraging because there was a close match amongst the results obtained by all the considered differencing schemes.

Of course second order scheme is much closer to the QUICK scheme which is considered very accurate in terms of prediction of transition flow, which is the type of flow under consideration. Further an experimental verification may be required of this numerical prediction.

ACKNOWLEDGEMENT

Authors acknowledge the cooperation extended by authorities of National Institute of Technology, Raipur (C.G.) INDIA for providing the licensed commercial software code ANSYS FLUENT (ANSYS Academic Research CFD version 12).

Also we acknowledge TecplotInc for providing Demo version of Teccplot360 for plotting some of the diagrams.

NOMENCLACTURE

Notation	Description of variables/Constants
D_H	Hydraulic mean Diameter, 2δ m
E	Eccentricity (Displacement of inner –cylinder axis from outer-cylinder axis), m
e_{max}	Maximum eccentricity, m
K	Consistency Index, Pa-s^n
N	Power-law index
P	Pressure, Pa
R	Radial distance from axis of inner-cylinder, m
R_i, D_i	Outer radius & diameter of inner-cylinder, m
R_O, D_O	Inner radius & diameter of outer cylinder, m
A	Cross sectional area of annulus of flow, $(\pi/4)$ ($D_O^2 - D_i^2$) m^2
Re	Bulk axial Reynolds number, $2\delta\rho U/\mu_{wall}$
U	Bulk axial velocity, m/s
U_{inlet}	Bulk axial velocity at inlet, m/s
U_a	Axial component of the velocity, m/s
U_t	Tangential component of velocity, m/s
U_r	Radial component of velocity, m/s
U_{rn}	Normailised radial velocity
U_{tn}	Normalised tangential velocity
U_{an}	Normalised axial velocity
R	Radial coordinate, m
z	Axial distance, m
A	Coordinate along axial (i.e. z-direction)
Φ	Angular location with respect to inner cylinder
T	Coordinate along angular direction (i.e. tangential coordinate)
P	Fluid Density, kg/m^3
μ	Characteristic Dynamic viscosity for flow, Pa-s
μ_{wall}	μ at wall, Pa-s
Ω	Angular velocity of inner cylinder, rad/s
O_1	Centre of inner cylinder (reference centre)
O_2	Centre of the outer cylinder
T	Time coordinate
□	Characteristic Shear Rate of flow (s^{-1})
σ_T	Reynolds stress
P	Flow pressure
e_r	Unit vector along radial coordinate
e_t	Unit vector along tangential coordinate
e_a	Unit vector along axial coordinate
$P1_X$	Distance along plane $P1$
$P2_Y$	Distance along plane $P2$
$P3_X$	Distance along plane $P3$
$P1_{nX}$	Normalised values in relation to $P1_X$
$P2_{nY}$	Normalised values in relation to $P2_{nY}$
$P3_{nX}$	Normalised values in relation to $P3_{nX}$

REFERENCES

[1]. J. M. Nouri and J. H. Whitelaw, Flow of Newtonian and non-Newtonian fluids in an eccentric annulus with rotation of inner cylinder, International Journal of Heat and Fluid Flow 18:236-246, 1997.

[2]. M. P. Escudier, P.J. Oliveira, F. T. Pinho (2002) Fully developed laminar flow of purely viscous non- Newtonian liquids through annuli, including the effects of eccentricity and inner-cylinder rotation. Int J Heat Fluid Flow 23:52–73.

[3]. D.O.A. Cruz and F.T. Pinho, Skewed Poiseuille –Couette Flowsof sPTTFluids in concentric annuli and channels, J. Non-Newtonian Fluid Mech. 121 (2004) 1–14.

[4]. I. A. Frigaard and G. A. Ngwa, Slumping Flows in Narrow Eccentric Annuli: Design of Chemical Packers and Cementing of Subsurface Gas Pipelines,Transp Porous Med ..... 2nd Order Upwind..... QUICK..... Power Law Comparison of Various Numerical Differencing Schemes in

Predicting Non-Newtonian Transition flow through an Eccentric Annulus with Inner Cylinder in Rotation International Conference on Advance in Mechanical and Industrial Engineering, 2 25 5th November 2012, Raipur, ISBN: 978-93-82208-39-6 45 (2010) 83:29–53 DOI 10.1007/s11242-009-9467-1, Springer Science + Business Media B.V. 2009.

[5]. V. C. Kelessidis (SPE) and G. E. Bandelis (Technical U. Of Crete), Flow Pattern and Minimum Suspension Velocity for Efficient Cuttings Transport in Horizontal and Deviated Wells in Coiled Tube Drilling, December 2004 SPE (Society of Petroleum Engineers), Drilling and Completion.

[6]. M. P. Escudier, P. J. Oliveira, F. T. Pinho, S. Smith, Fully Developed Lamiar Flow of Non-Newtonian liquids through annuli: Comparison of numerical calculations with experiments; Experiments in Fluids 33 (2002) 101 – 111.

[7]. H. K. Versteeg and W. Malalasekhara, An Introduction to Computational Fluid Dynamics (The Finite Volume method), Second Edition, Pearson Education Ltd.

[8]. ANSYS Academic Research CFD version 12 user guide & Manuals.

[9]. K. Muralidhar& G. Biswas, Advanced Engineering Fluid Mechanics, Second Edition, Narosa Publishing House Pvt. Ltd.

[10]. A. A. Gavrilov, A.V.Minakov, A.A.Dekterev, and V. Ya. Rudyak; A Numerical Algorithm for Modeling Laminar Flows in an Annular Channel with Eccentricity; Journal of Applied and Industrial Mathematics, 2011, Vol. 5, No. 4, pp. 559–568.Pleiades Publishing, Ltd., 2011.

[11]. Sang-Mok Han, Young-Ju Kim, Nam-Sub Woo and Young-Kyu Hwang; A study on the solid-liquid 2 phase helical flow in an inclined annulus; Journal of Mechanical Science and Technology 22 (2008) 1914-1920.

[12]. Wang Zhiyuan and Sun Baojiang; Annular multiphase flow behavior during deep water drilling and the effect of hydrate phase transition; Pet. Sci. (2009) 6:57-63.

[13]. Young-Ju Kim and Young-Kyu Hwang; Experimental Study on the Vortex Flow in a Concentric Annulus with a rotating inner cylinder; KSME International Journal, Vol. 17 No. 4, pp. 562~570, 2003.

[14]. E. V. Podryabinkin and V. Ya. Rudyak; Moment and Forces Exerted on the Inner Cylinder in Eccentric Annular flow; Journal of Engineering Thermophysics, 2011, Vol. 20, No. 3, pp. 320–328. Pleiades Publishing, Ltd., 2011.

[15]. Sang-mok Han, Nam-sub Woo, and Young-kyu Hwang; Solid-liquid mixture flow through a slim hole annulus with rotating inner cylinder; Journal of Mechanical Science and Technology 23 (2009) 569~577.